

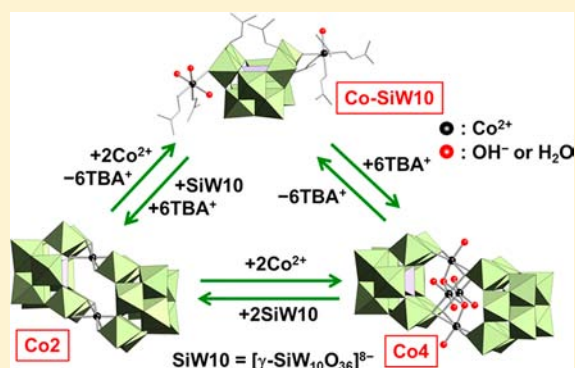
Synthesis, Structure Characterization, and Reversible Transformation of a Cobalt Salt of a Dilacunary γ -Keggin Silicotungstate and Sandwich-Type Di- and Tetracobalt-Containing Silicotungstate Dimers

Yuji Kikukawa, Kosuke Suzuki, Kazuya Yamaguchi, and Noritaka Mizuno*

Department of Applied Chemistry, School of Engineering, The University of Tokyo, 7-3-1 Hongo, Bunkyo-ku, Tokyo 113-8656, Japan

Supporting Information

ABSTRACT: A cobalt salt of a γ -Keggin dilacunary silicotungstate, $\{\text{CoL}_5\}_2[\gamma\text{-SiW}_{10}\text{O}_{34}\text{L}_2]$ [**Co-SiW10**; L = *N,N*-dimethylformamide (DMF) or H_2O], could be synthesized by the cation-exchange reaction of $\text{TBA}_4[\gamma\text{-H}_4\text{SiW}_{10}\text{O}_{36}]$ (TBA = tetra-*n*-butylammonium) with 2 equiv of $\text{Co}(\text{NO}_3)_2$ with respect to $\text{TBA}_4[\gamma\text{-H}_4\text{SiW}_{10}\text{O}_{36}]$ in a mixed solvent of DMF and acetone (97% yield). Each **Co-SiW10** was linked by water molecules via a hydrogen-bonding network. Besides **Co-SiW10**, various kinds of isostructural **M-SiW10** could be synthesized via the same procedure as that for **Co-SiW10** ($M = \text{Mn}^{2+}, \text{Fe}^{2+}, \text{Ni}^{2+}, \text{Cu}^{2+}, \text{Zn}^{2+}, \text{and Cd}^{2+}$). By the reaction of **Co-SiW10** with 1 equiv of $\text{TBA}_6[\gamma\text{-H}_2\text{SiW}_{10}\text{O}_{36}]$ in acetone, a silicotungstate dimer pillared by two cobalt cations with a significantly slipped dimer configuration, $\text{TBA}_6[\text{Co}_2(\gamma\text{-H}_3\text{SiW}_{10}\text{O}_{36})_2]\cdot 3\text{H}_2\text{O}$ (**Co2**), could be synthesized. By the reaction of **Co-SiW10** with 3 equiv of TBAOH in acetone, a tetracobalt-containing sandwich-type silicotungstate, $\text{TBA}_6[\{\text{Co}(\text{H}_2\text{O})\}_2(\mu_3\text{-OH})_2\{\text{Co}(\text{H}_2\text{O})\}_2(\gamma\text{-H}_2\text{SiW}_{10}\text{O}_{36})_2]\cdot 5\text{H}_2\text{O}$ (**Co4**), could be synthesized. Compound **Co4** possessed the tetracobalt–oxygen core, $[\{\text{Co}(\text{H}_2\text{O})\}_2(\mu_3\text{-OH})_2\{\text{Co}(\text{H}_2\text{O})\}_2]^{6+}$, identical with those of previously reported Weakley-type sandwich polyoxometalates, $[\text{Co}_4(\text{H}_2\text{O})_2(\text{XM}_9\text{O}_{34})_2]^{n-}$ ($X = \text{P}^{5+}, \text{Si}^{4+}, \text{Ge}^{4+}, \text{As}^{5+}$ or V^{5+} ; $M = \text{Mo}^{6+}$ or W^{6+}). The reversible transformation between these three compounds (**Co-SiW10** \rightleftharpoons **Co2**, **Co-SiW10** \rightleftharpoons **Co4**, and **Co2** \rightleftharpoons **Co4**) took place by the addition and/or subtraction of required components in appropriate solvents, affording the desired products in high yields (71–93% yields).



INTRODUCTION

Polyoxometalates (POMs) are anionic metal–oxygen clusters of highly oxidized early transition metals and have stimulated many current research activities in broad fields of science such as analytical chemistry, medicinal chemistry, electrochemistry, photochemistry, and catalyst chemistry.¹ Their chemical and physical properties can precisely be tuned by selecting constituent elements and counteranions.¹ In particular, the introduction of sophisticated metal cores into the POM frameworks has an essential role in controlling their redox,^{1a} magnetic,^{1b–d} optical,^{1e} and catalytic properties.^{1f–k}

It has been reported that multimetal-substituted or -encapsulated POMs show unique catalytic^{2,3} and magnetic properties.^{4,5} In particular, much attention has been paid to the synthesis of multicobalt-containing POMs because they can act as efficient photocatalysts for decoloration/degradation of dyes (e.g., Acid Orange 7),^{2a} water oxidation catalysts,^{2b} and single-molecule magnets with unique magnetic behaviors.⁴ Up to now, various kinds of cobalt-containing POMs have been reported (Tables S1 and S2 in the Supporting Information, SI);^{4–16} for example, mono- and tricobalt-substituted Keggin and Dawson

monomers,⁶ mono- to tetracobalt-containing sandwich-type Keggin dimers,⁷ mono- to tetracobalt-containing Dawson dimers,⁸ mono- to tricobalt-containing open Dawson-type POMs (Keggin dimers),⁹ banana-shaped two tricobalt-containing Keggin dimers, $([\{\text{Co}_3(\text{H}_2\text{O})\}_2(\text{XW}_6\text{O}_{26})(\text{XW}_9\text{O}_{34})_2]^{n-})$,¹⁰ multicobalt-containing Keggin and Dawson multimers,¹¹ and their derivatives with cobalt cations modified with organic or phosphate ligands.¹² Although some cobalt-containing Keggin POMs, e.g., $[\text{Co}_4(\text{H}_2\text{O})_2(\text{PW}_9\text{O}_{34})_2]^{10-}$, $[\{\text{Co}_3(\text{H}_2\text{O})\}_2(\text{AsW}_6\text{O}_{26})(\text{AsW}_9\text{O}_{34})_2]^{17-}$, $[\text{Co}_9(\text{OH})_3(\text{H}_2\text{O})_6(\text{HPO}_4)_2(\text{PW}_9\text{O}_{34})_3]^{16-}$, and $[\text{H}_{19}\text{Co}_{2.5}(\text{W}_{3.5}\text{O}_{14})(\text{SeW}_9\text{O}_{33})\text{-}(\text{Se}_2\text{W}_{30}\text{O}_{107})]^{17-}$, can simply be synthesized by the mixing of metal salts [e.g., Na_2WO_4 , $\text{Co}(\text{NO}_3)_2$, Na_2HPO_4 , NaHAsO_4 , and/or K_2SeO_3], the precise design and prediction of structures are very difficult.¹³ On the other hand, isolated lacunary POMs have often been utilized as rigid multidentate oxygen-donor ligands to synthesize controlled metal–oxygen cores by substitution into the lacunary pockets or encapsulation within

Received: April 2, 2013

Published: July 8, 2013



two or more lacunary POMs.¹⁴ However, the reaction of dilacunary γ -Keggin POMs, $[\gamma\text{-XW}_{10}\text{O}_{36}]^{8-}$ ($X = \text{Si}^{4+}$ or Ge^{4+}), with cobalt cations in aqueous media has typically afforded unexpected structures because their isomerization and/or decomposition very easily proceed upon heating in acidic aqueous media containing cobalt cations; for example, $[\text{Co}(\text{H}_2\text{O})_2\{\text{Co}_3(\text{B}-\beta\text{-GeW}_9\text{O}_{33}(\text{OH}))(\text{B}-\beta\text{-GeW}_8\text{O}_{30}(\text{OH}))\}_2]^{22-}$, $[\text{Co}_3(\text{H}_2\text{O})(\text{B}-\beta\text{-SiW}_9\text{O}_{34})(\text{B}-\beta\text{-SiW}_8\text{O}_{29}(\text{OH}))]^{12-}$, $[\text{Co}_3(\text{H}_2\text{O})(\text{B}-\alpha\text{-SiW}_9\text{O}_{34})(\text{B}-\beta\text{-SiW}_8\text{O}_{31})]^{14-}$, $[\text{Co}_2\text{Cl}_2(\text{OH})_3(\text{H}_2\text{O})_9(\text{B}-\beta\text{-SiW}_8\text{O}_{31})_3]^{17-}$, $[\text{Co}(\text{H}_2\text{O})_2\{\text{Co}_3(\text{H}_2\text{O})(\text{B}-\beta\text{-SiW}_9\text{O}_{33}(\text{OH}))(\beta\text{-SiW}_8\text{O}_{29}(\text{OH}))\}_2]^{20-}$, $[\text{Co}_{1.5}(\text{H}_2\text{O})_7][\text{Co}_4(\text{OH})(\text{H}_2\text{O})_7(\gamma\text{-SiW}_{10}\text{O}_{36})(\beta\text{-SiW}_8\text{O}_{30}(\text{OH}))]^{7-}$, $[\{\beta\text{-SiCo}_2\text{W}_{10}\text{O}_{36}(\text{OH})_2(\text{H}_2\text{O})\}_2]^{12-}$, $[\text{Co}_6(\text{H}_2\text{O})_{30}\{\text{Co}_9\text{Cl}_2(\text{OH})_3(\text{H}_2\text{O})_9(\beta\text{-SiW}_8\text{O}_{31})_3\}]^{5-}$, $[\{\text{Co}_3(\text{B}-\beta\text{-SiW}_9\text{O}_{33}(\text{OH}))(\text{B}-\beta\text{-SiW}_8\text{O}_{29}(\text{OH}))\}_2]^{22-}$, $[\text{Co}_2(\text{H}_2\text{O})_{10}\text{Co}_4(\text{H}_2\text{O})_2(\text{B}-\alpha\text{-XW}_9\text{O}_{34})_2]^{8-}$ ($X = \text{Si}^{4+}$ or Ge^{4+}), $[\text{Co}(\text{H}_2\text{O})_3(\alpha\text{-GeW}_{11}\text{CoO}_3)]^{10-}$, and $[\text{Co}_4(\text{H}_2\text{O})_2(\text{SiW}_9\text{O}_{34})_2]^{12-}$ have been synthesized with $\text{K}_8[\gamma\text{-XW}_{10}\text{O}_{36}]$ (Table S2 in the SI).¹⁵ Although a cobalt-containing γ -Keggin sandwich-type POM, $[\{\text{K}(\text{H}_2\text{O})_2\text{Co}(\text{H}_2\text{O})_2(\gamma\text{-SiW}_{10}\text{O}_{36})_2\}]^{8-}$, has successfully been synthesized with $\text{K}_8[\gamma\text{-SiW}_{10}\text{O}_{36}]$ in an aqueous medium without isomerization and decomposition of the γ -Keggin POM framework, this POM possesses only one cobalt cation with respect to two $[\gamma\text{-SiW}_{10}\text{O}_{36}]^{8-}$ subunits.¹⁶ In this case, potassium cations exist around vacant sites of the lacunary $[\gamma\text{-SiW}_{10}\text{O}_{36}]^{8-}$ and inhibit the introduction of multicobalt cores.¹⁶ To the best of our knowledge, the successful synthesis of multicobalt-containing γ -Keggin POMs has never been reported to date.

Recently, we have successfully developed novel synthetic procedures for multimetal-containing γ -Keggin POMs in organic media without using alkali-metal salts of the lacunary POM precursor [typically using the tetra-*n*-butylammonium (TBA) salt].¹⁷ In this paper, we report that a cobalt salt of a γ -Keggin silicotungstate, $\{\text{CoL}_5\}_2[\gamma\text{-SiW}_{10}\text{O}_{34}\text{L}_2]$ [**Co-SiW10**; L = *N,N*-dimethylformamide (DMF) or H_2O], can successfully be synthesized by the cation-exchange reaction of $\text{TBA}_4[\gamma\text{-H}_4\text{SiW}_{10}\text{O}_{36}]$ with $\text{Co}(\text{NO}_3)_2$ in a mixed solvent of DMF and acetone. In addition, **Co-SiW10** is used as a precursor for sandwich-type di- and tetracobalt-containing γ -Keggin silicotungstate dimers, $\text{TBA}_6[\text{Co}_2(\gamma\text{-H}_3\text{SiW}_{10}\text{O}_{36})_2]$ (**Co2**) and $\text{TBA}_6[\{\text{Co}(\text{H}_2\text{O})\}_2(\mu_3\text{-OH})_2\{\text{Co}(\text{H}_2\text{O})_2\}_2(\gamma\text{-H}_2\text{SiW}_{10}\text{O}_{36})_2]$ (**Co4**). The synthesis, structure characterization, and reversible transformation (**Co-SiW10** \rightleftharpoons **Co2**, **Co-SiW10** \rightleftharpoons **Co4**, and **Co2** \rightleftharpoons **Co4**) of these three POMs are also discussed in detail.

EXPERIMENTAL SECTION

General Procedures. Thermogravimetric and differential thermal analyses (TG-DTA) were performed on a Rigaku Thermo plus TG 8120. IR spectra were measured on a Jasco FT/IR-4100 using KBr disks. Diffuse-reflectance UV/vis spectra were measured on a Jasco V-570DS. Powder X-ray diffraction (XRD) patterns were measured with a XRD multiflex [Rigaku, 40 kV/50 mA, Cu K α radiation ($\lambda = 1.5405 \text{ \AA}$)]. Inductively coupled plasma atomic emission spectroscopy analyses were performed on a Shimadzu ICPS-8100. Magnetic measurements were performed on a Quantum Design MPMS-XL7 operating between 1.9 and 300 K under a 1000 Oe magnetic field. Diamagnetic correction for **Co-SiW10** was applied by the sample holder (polycarbonate) and $[\text{ZnL}_5]_2[\gamma\text{-SiW}_{10}\text{O}_{34}\text{L}_2]$ (**Zn-SiW10**; L = DMF or H_2O), and those for **Co2** and **Co4** were applied by the sample holder and $\text{TBA}_4[\gamma\text{-H}_4\text{SiW}_{10}\text{O}_{36}]$. Cyclic voltammetric measurements were carried out with a Solartron SI 1287 Electrochemical Interface.¹⁸ A standard three-electrode arrangement was

employed with a BAS glassy carbon disk electrode as the working electrode, a platinum wire as the counter electrode, and a Ag/AgCl as the reference electrode for an aqueous medium or a silver wire electrode as the pseudoreference electrode for an organic medium. The voltage scan rate was set at 100 mV s^{-1} . The potentials in all voltammetric experiments were converted using data derived from the oxidation of Fc [Fc/Fc^+ (Fc = ferrocene)] as an external reference. $\text{TBA}_4[\gamma\text{-H}_4\text{SiW}_{10}\text{O}_{36}]\cdot\text{H}_2\text{O}$ and $\text{TBA}_6[\gamma\text{-H}_3\text{SiW}_{10}\text{O}_{36}]$ were synthesized according to the reported procedures.¹⁹

Synthesis of Co-SiW10. $\text{TBA}_4[\gamma\text{-H}_4\text{SiW}_{10}\text{O}_{36}]\cdot\text{H}_2\text{O}$ (1.0 g, 0.29 mmol) was dissolved in a mixed solvent of DMF and acetone (20 mL, 1:1, v/v), and then $\text{Co}(\text{NO}_3)_2\cdot 6\text{H}_2\text{O}$ (0.17 g, 0.58 mmol) was added. The resulting solution was stirred for 15 min at room temperature (ca. 293 K). The pink precipitates formed were filtered off, washed with acetone, and dried to afford 0.98 g of **Co-SiW10** (97% yield based on $\text{TBA}_4[\gamma\text{-H}_4\text{SiW}_{10}\text{O}_{36}]$). Recrystallization of **Co-SiW10** from a mixed solvent of water, DMF, and acetone (1:1:1, v/v/v, kept overnight at 253 K) gave pink crystals suitable for X-ray crystallographic analysis. Anal. Calcd for $\{\text{Co}(\text{DMF})_2(\text{H}_2\text{O})_3\}\{\text{Co}(\text{DMF})_4(\text{H}_2\text{O})\}[\gamma\text{-SiW}_{10}\text{O}_{34}(\text{DMF})_2]\cdot 2\text{DMF}\cdot 11\text{H}_2\text{O}$: C, 10.31; H, 2.77; N, 4.01; Si, 0.80; W, 52.62; Co, 3.37. Found: C, 10.11; H, 2.43; N, 3.56; Si, 0.80; W, 52.94; Co, 3.48. IR (KBr pellet; $4000\text{--}300 \text{ cm}^{-1}$): 3420, 2938, 2814, 1653, 1496, 1436, 1381, 1361, 1251, 1115, 1062, 998, 961, 879, 850, 781, 700, 668, 604, 568, 544, 494, 457, 405, 361, 351, 335, 312, 300.

Transformation of Co-SiW10 into Co2. Compound **Co-SiW10** (49 mg, 0.014 mmol) was immersed in acetone (1.5 mL), followed by the addition of $\text{TBA}_6[\gamma\text{-H}_3\text{SiW}_{10}\text{O}_{36}]$ (55 mg, 0.014 mmol), giving a yellow solution. The solution was stirred for 1 h at room temperature (ca. 303 K). Then, the yellow precipitates formed were filtered off, washed with acetone, and dried to afford 65 mg of **Co2** (71% yield based on **Co-SiW10**). Recrystallization of **Co2** from a mixed solvent of nitromethane and diethyl ether (1:2, v/v, kept for a few hours at 303 K) gave yellow crystals suitable for X-ray crystallographic analysis. Anal. Calcd for $\text{TBA}_6[\text{Co}_2(\gamma\text{-H}_3\text{SiW}_{10}\text{O}_{36})_2]\cdot 3\text{H}_2\text{O}$: C, 17.69; H, 3.53; N, 1.29; Si, 0.86; W, 56.41; Co, 1.81. Found: C, 17.84; H, 3.55; N, 1.17; Si, 0.88; W, 56.83; Co, 1.58. IR (KBr pellet; $4000\text{--}300 \text{ cm}^{-1}$): 3447, 2962, 2874, 1483, 1381, 1153, 1106, 1066, 1001, 968, 883, 784, 668, 600, 555, 457, 392, 385, 361, 356, 334, 310, 302.

Transformation of Co2 into Co-SiW10. Compound **Co2** (95 mg, 0.0145 mmol) was dissolved in a mixed solvent of DMF and acetone (2 mL, 1:1, v/v), and then $\text{Co}(\text{NO}_3)_2\cdot 6\text{H}_2\text{O}$ (8.5 mg, 0.029 mmol) and HNO_3 (1 M aqueous solution, 0.029 mL, 0.029 mmol) were added. The resulting solution was stirred for 15 min at room temperature (ca. 293 K). The pink precipitates formed were filtered off, washed with acetone, and dried to afford 95 mg of **Co-SiW10** (93% yield based on **Co2**).

Transformation of Co-SiW10 into Co4. Compound **Co-SiW10** (100 mg, 0.029 mmol) was immersed in acetone (1.5 mL), followed by the addition of TBAOH (40% aqueous solution, 56 mg, 0.087 mmol), giving a purple solution. The solution was stirred for 40 min at 303 K. Then, the purple precipitates formed were filtered off, washed with acetone, and dried to afford 86 mg of **Co4** (87% yield based on **Co-SiW10**). The synthetic solution was filtered just after the addition of TBAOH, and the filtrate was kept for a few hours at 303 K, giving purple crystals suitable for X-ray crystallographic analysis. Anal. Calcd for $\text{TBA}_6[\{\text{Co}(\text{H}_2\text{O})\}_2(\mu_3\text{-OH})_2\{\text{Co}(\text{H}_2\text{O})_2\}_2(\gamma\text{-H}_2\text{SiW}_{10}\text{O}_{36})_2]\cdot 5\text{H}_2\text{O}$: C, 16.93; H, 3.61; N, 1.23; Si, 0.82; W, 53.98; Co, 3.46. Found: C, 17.16; H, 3.79; N, 1.48; Si, 0.80; W, 54.30; Co, 3.38. IR (KBr pellet; $4000\text{--}300 \text{ cm}^{-1}$): 3424, 2961, 2935, 2873, 1658, 1485, 1380, 1253, 1152, 1087, 998, 957, 892, 770, 555, 457, 361, 338, 310.

Transformation of Co4 into Co-SiW10. Compound **Co4** (99 mg, 0.0145 mmol) was dissolved in a mixed solvent of DMF and acetone (2 mL, 1:1, v/v), and then HNO_3 (1 M aqueous solution, 0.087 mL, 0.087 mmol) was added. The resulting solution was stirred for 15 min at room temperature (ca. 293 K). The pink precipitates formed were filtered off, washed with acetone, and dried to afford 92 mg of **Co-SiW10** (91% yield based on **Co4**).

Transformation of Co2 into Co4. Compound Co2 (98 mg, 0.015 mmol) was immersed in acetone (1.5 mL), followed by the addition of DMF (22 mg, 0.30 mmol), H₂O (28 mg, 1.6 mmol), and Co(acac)₂·2H₂O (8.8 mg, 0.030 mmol; acac = acetylacetonato), giving a purple solution. The solution was stirred for 40 min at 303 K. Then, the purple precipitates formed were filtered off, washed with acetone, and dried to afford 85 mg of Co4 (85% yield based on Co2).

Transformation of Co4 into Co2. Compound Co4 (51 mg, 0.0075 mmol) was dissolved in nitromethane (0.5 mL), and then acetone (1.0 mL) was added. The addition of TBA₄[γ -H₄SiW₁₀O₃₆]·H₂O (52 mg, 0.015 mmol) and *p*-toluenesulfonic acid monohydrate (2.9 mg, 0.015 mmol) gave a yellow solution. Acetone (4 mL) was further added to the solution, and the resulting solution was stirred for 1 h at 303 K. Then, the yellow precipitates formed were filtered off, washed with acetone, and dried to afford 72 mg of Co2 (74% yield based on Co4).

Synthesis of Co2Zn2 with Co2 and Zn(acac)₂. Compound Co2 (98 mg, 0.015 mmol) was immersed in acetone (3 mL), followed by the addition of Zn(acac)₂ (7.9 mg, 0.030 mmol), TBAOH (40% aqueous solution, 20 mg, 0.030 mmol), and H₂O (38 mg, 2.1 mmol), giving a pink solution. To the solution was added ethyl acetate (3 mL), and the resulting solution was stirred for 10 min at room temperature (ca. 293 K). Then, the pink precipitates formed were filtered off, washed with ethyl acetate, and dried to afford 84 mg of Co2Zn2 (78% yield based on Co2).

X-ray Crystallographic Analysis. Diffraction measurements were made on a Rigaku MicroMax-007 Saturn 724 CCD detector with graphite-monochromated Mo K α radiation ($\lambda = 0.71069$ Å) at 123 K. Data were collected and processed using *CrystalClear*²⁰ for Windows software and *HKL2000*²¹ for Linux software. Neutral scattering factors were obtained from the standard source. In the reduction of data, Lorentz and polarization corrections were made. The structure analysis was performed using *CrystalStructure*²² and *Win-GX*²³ for Windows software. All structures were solved by *SHELXS-97* (direct methods) and refined by *SHELXL-97*.²⁴ The data set for Co2 was improved by using the *ACTA 50* command. The metal atoms (silicon, tungsten, cobalt and zinc) were refined anisotropically, and the carbon, oxygen, and nitrogen atoms were refined isotropically. Hydrogen atoms were excluded from the structural solutions. TBA cations and DMF, acetone, and nitromethane molecules were partly disordered over two positions. The details are described in the SI. CCDC 929364 (Co-SiW10), 929365 (Co2), and 929366 (Co4) contain the supplementary crystallographic data for this paper. These data can be obtained free of charge from The Cambridge Crystallographic Data Centre or the SI of this paper.

RESULTS AND DISCUSSION

Synthesis and Structure Characterization of Co-SiW10. By the reaction of TBA₄[γ -H₄SiW₁₀O₃₆] with 2 equiv of Co(NO₃)₂ with respect to TBA₄[γ -H₄SiW₁₀O₃₆] in a mixed solvent of DMF and acetone (1:1, v/v), the pink precipitates of Co-SiW10 were obtained in an almost quantitative yield (97% yield based on TBA₄[γ -H₄SiW₁₀O₃₆]). The IR band positions of Co-SiW10 in the fingerprint region of the POM framework (1200–500 cm⁻¹) were almost identical with those of TBA₄[γ -H₄SiW₁₀O₃₆] (Figure 1b), showing that Co-SiW10 maintains the γ -Keggin POM framework. By the reaction of TBA₄[γ -H₄SiW₁₀O₃₆] with Co(NO₃)₂, the intensities of the C–H stretching vibrations (around 2900 cm⁻¹) much decreased (Figure 1b), suggesting that TBA cations are exchanged with cobalt cations. The C=O stretching vibration of DMF was observed at 1653 cm⁻¹ and was red-shifted in comparison with that of noncoordinated DMF (1678 cm⁻¹), showing coordination to the metal cations.²⁵ The diffuse-reflectance UV/vis spectrum of Co-SiW10 showed a broad band at 528 nm assignable to the d–d transition of the octahedral Co²⁺ cations (Figure 2b).²⁶

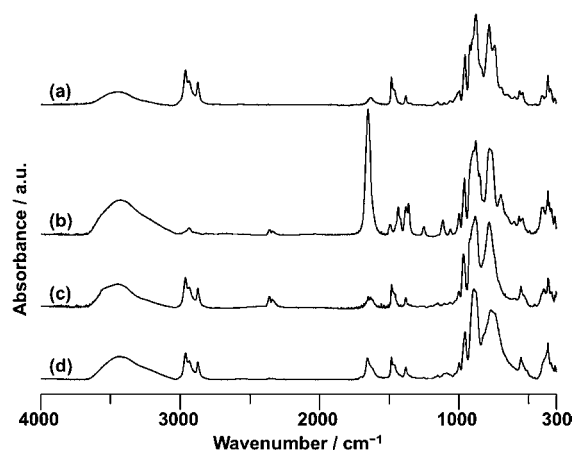


Figure 1. IR spectra (in the range of 300–4000 cm⁻¹) of (a) TBA₄[γ -H₄SiW₁₀O₃₆], (b) Co-SiW10, (c) Co2, and (d) Co4.

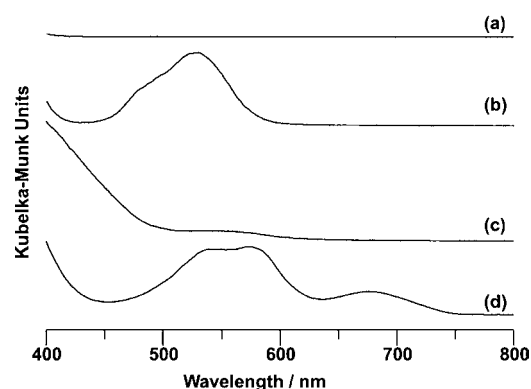


Figure 2. Diffuse-reflectance UV/vis spectra (in the range of 400–800 nm) of (a) TBA₄[γ -H₄SiW₁₀O₃₆], (b) Co-SiW10, (c) Co2, and (d) Co4.

The single crystals of Co-SiW10 suitable for X-ray crystallographic analysis were successfully obtained by recrystallization from a mixed solvent of water, DMF, and acetone. The molecular structure is represented in Figure 3 (Figure S1 in the SI for ORTEP and Table S3 in the SI for the crystallographic data). The selected bond lengths are summarized in Table 1. Compound Co-SiW10 was a discrete dilacunar γ -Keggin silicotungstate monomer with two cobalt cations, which were not located at the vacant sites but near the POM framework. The bond-valence-sum (BVS) values of cobalt (2.03 and 2.08), tungsten (5.92–6.17), and silicon (4.31) atoms in Co-SiW10 indicate that the respective valences are 2+, 6+, and 4+.²⁷ Two DMF molecules existed on the axial positions of tungsten atoms W2 and W3, resulting in distortion of the γ -Keggin POM framework in comparison with those of previously reported POMs.²⁸ Cobalt cations were connected to the equatorial terminal oxygen atoms of W1 and W4 (O7 and O12). Each cobalt cation was octahedrally coordinated to five external ligands (H₂O and DMF) and one oxygen atom of the POM framework. The data of X-ray, elemental, and TG analyses show that the formula of Co-SiW10 is {Co(DMF)₂(H₂O)₃}{Co(DMF)₄(H₂O)}[γ -SiW₁₀O₃₄(DMF)₂]·2DMF·11H₂O. The formation of Co-SiW10 can be expressed by eq 1.

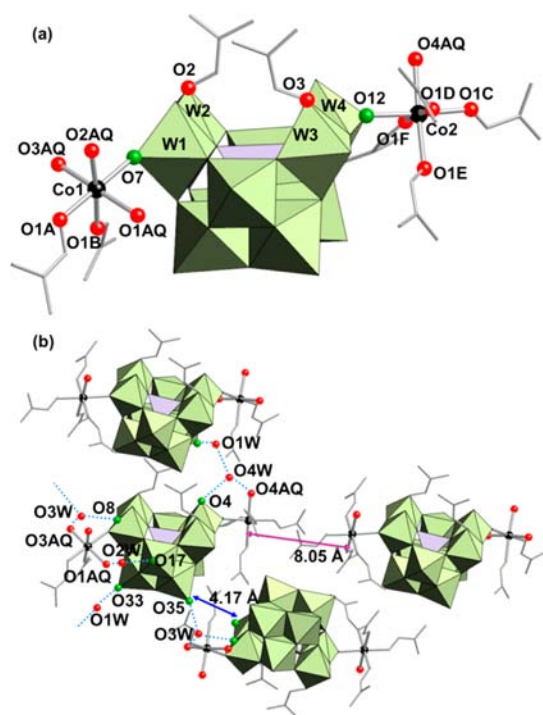
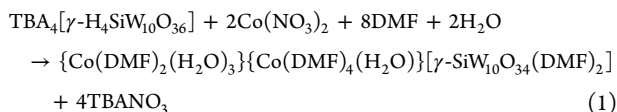


Figure 3. Polyhedral and ball-and-stick representation of **Co-SiW10**: (a) single molecule (see Figure S1 in the SI for ORTEP); (b) representative drawing of the hydrogen-bonding network between **Co-SiW10** molecules. The $\{\text{WO}_6\}$ and $\{\text{SiO}_4\}$ units are shown as green octahedra and gray tetrahedra, respectively. Black, red, and green spheres indicate cobalt cations, oxygen atoms of aqua ligands or DMF molecules, and oxygen atoms of the $\{\text{WO}_6\}$ units, respectively. Blue dotted lines show the hydrogen-bonding interactions. Pink and blue arrows show the distance of the closest cobalt cations (8.05 Å) and the closest oxygen atoms of **Co-SiW10** (4.17 Å), respectively. Lattice DMF and acetone molecules are omitted for clarity.

Table 1. Selected Bond Lengths (Å) for **Co-SiW10**

Co1...Co2	15.619	Co2...Co2	8.047
Co1–O7	2.092	Co1–O AQ	2.106
Co1–O _{DMF}	2.075	Co2–O12	2.096
Co2–O4AQ	2.096	Co1–O _{DMF}	2.079
O1W...O33	2.846	O1W...O08	2.806
O2W...O01	2.675	O2W...O17	2.861
O3W...O03	2.737	O3W...O08	2.774
O3W...O35	2.817	O4W...O04	2.746
O4W...O4	2.798		



Besides **Co-SiW10**, various kinds of divalent metal salts of lacunary γ -Keggin silicotungstates **M-SiW10** could be synthesized via the same procedure as that for **Co-SiW10** ($M = \text{Mn}^{2+}$, Fe^{2+} , Ni^{2+} , Cu^{2+} , Zn^{2+} , or Cd^{2+} ; typically >95% yields based on $\text{TBA}_4[\gamma\text{-H}_4\text{SiW}_{10}\text{O}_{36}]$; Figure S2 in the SI). While alkali metal (e.g., K^+ , Rb^+ , or Cs^+)²⁹ and alkylammonium salts of the lacunary γ -Keggin silicotungstates¹⁹ have been synthesized to date, the transition-metal salts of **M-SiW10** have never been reported.

Compound **Co-SiW10** exhibited an extensive hydrogen-bonding network among the lattice water molecules (O1W,

O3W, and O4W), aqua ligands (O1AQ, O3AQ, and O4AQ), and oxygen atoms of POM frameworks (O4, O8, O17, O33, and O35) (blue dotted lines in Figure 3b, with distances of 2.675–2.861 Å; Table 1).³⁰ Each **Co-SiW10** was linked by water molecules (O1W, O3W, and O4W) via the hydrogen-bonding network but separated at least by 4.17 Å (blue arrow in Figure 3b).

The magnetic measurement of **Co-SiW10** was carried out using the polycrystalline sample (applied magnetic field 1000 Oe, 1.9–300 K; Figure 4a).^{31,32} The χT value of **Co-SiW10** at

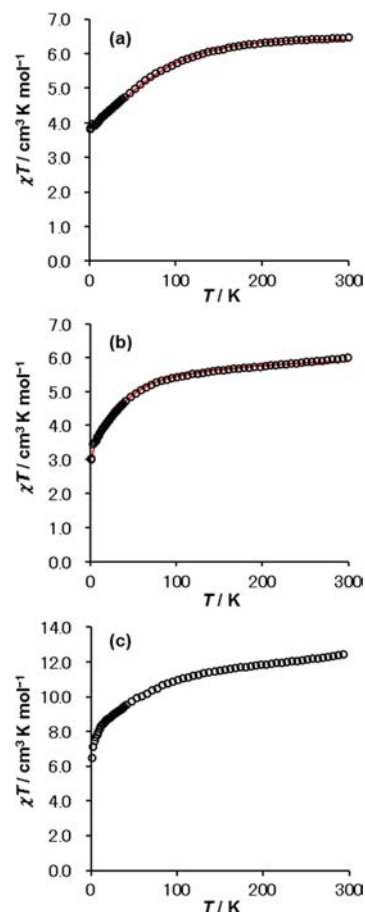


Figure 4. Temperature dependence of the χT product for polycrystalline samples of (a) **Co-SiW10**, (b) **Co2**, and (c) **Co4** in the temperature range of 1.9–300 K under a 1000 Oe field. Red solid lines in parts a and b represent the fitting data.^{33,34}

300 K was $6.46 \text{ cm}^3 \text{ K mol}^{-1}$ ($\mu_{\text{eff}} = 7.19 \mu_{\text{B}}$). This value was larger than the spin-only one of two high-spin Co^{2+} cations ($3.76 \text{ cm}^3 \text{ K mol}^{-1}$, $5.68 \mu_{\text{B}}$; $\mu_{\text{SO}} = [4S(S+1)]^{1/2}$; $S = 3/2$) and close to the value expected when the spin and orbital momentums independently exist ($6.76 \text{ cm}^3 \text{ K mol}^{-1}$, $7.35 \mu_{\text{B}}$; $\mu_{\text{LS}} = [L(L+1) + 4S(S+1)]^{1/2}$; $L = 3$, $S = 3/2$), indicating the contribution of the orbital momentum typical for a 4T_{1g} ground state. The intramolecular $\text{Co1}\cdots\text{Co2}$ distance was 13.7 Å, and the shortest intermolecular $\text{Co}\cdots\text{Co}$ distance (pink arrow in Figure 3b) was 8.07 Å. These long distances suggest that the magnetic interaction between cobalt cations can be neglected. Therefore, the decrease in the χT value with a decrease in temperature would be caused by the intrinsic spin–orbital coupling of the high-spin Co^{2+} cations.³³

Synthesis and Structure Characterization of Co2 and Reversible Transformation between Co-SiW10 and Co2.

By the reaction of Co-SiW10 with 1 equiv of TBA₆[γ -H₂SiW₁₀O₃₆] with respect to Co-SiW10 in acetone, the yellow precipitates of Co2 could be obtained (71% yield based on Co-SiW10). The IR bands assignable to TBA cations in Co2 were clearly observed at 2962, 2874, 1483, and 1381 cm⁻¹, and those assignable to DMF were not observed (Figure 1c). The IR band positions of Co2 in the fingerprint region (1200–500 cm⁻¹) of the POM framework were almost the same as those of TBA₄[γ -H₄SiW₁₀O₃₆] (Figure 1c), showing that Co2 possesses the γ -Keggin POM framework. The diffuse-reflectance UV/vis spectrum of Co2 showed a weak band around 550 nm (Figure 2c).

The single crystals of Co2 suitable for X-ray crystallographic analysis were successfully obtained by recrystallization from a mixed solvent of nitromethane and diethyl ether. The molecular structure of the anion part is represented in Figure 5 (Figure S3 in the SI for ORTEP and Table S3 in the SI for

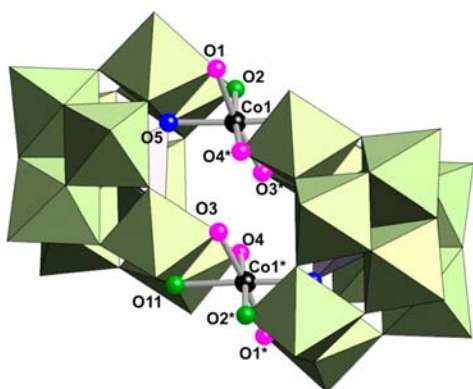


Figure 5. Polyhedral and ball-and-stick representation of the anion part of Co2 (see Figure S3 in the SI for ORTEP). The {WO₆} and {SiO₄} units are shown as green octahedra and gray tetrahedra, respectively. Black, green, pink, and blue spheres indicate cobalt cations, nonprotonated oxygen atoms of the {WO₆} units, monoprotinated oxygen atoms of the {WO₆} units, and oxygen atoms of the {SiO₄} units, respectively.

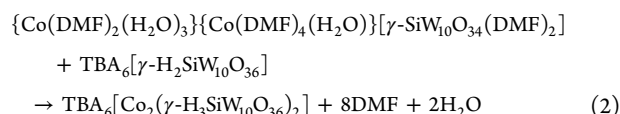
the crystallographic data). The selected bond lengths are summarized in Table 2. Six TBA cations per one Co2 anion

Table 2. Selected Bond Lengths (Å) for Co2

Co1...Co1*	5.14	Co1–O1	2.05
Co1–O2	2.05	Co1–O3*	2.06
Co1–O4*	2.03	Co1–O5	2.17
Co1–O11	2.29	O3...O4*	2.63

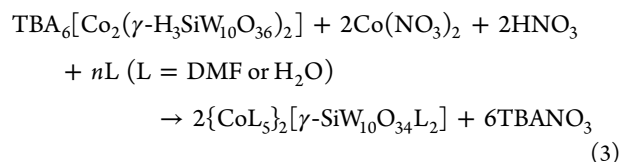
could crystallographically be assigned in accordance with the results of elemental analysis. The BVS values of the cobalt (1.97–2.03), tungsten (5.90–6.24), and silicon (3.86–3.93) atoms in Co2 indicate that the respective valences are 2+, 6+, and 4+. The χT value of Co2 at 300 K (5.99 cm³ K mol⁻¹; $\mu_{\text{eff}} = 6.92 \mu_{\text{B}}$; Figure 4b) was close to that calculated with two Co²⁺ cations upon the independent existence of the spin and orbital momentums (see the former section), indicating the contribution of the orbital momentum typical for a ⁴T_{1g} ground state.^{31,32,34} The BVS values of O1 (1.24), O3 (1.06), and O4 (1.16) were relatively lower than those of the other oxygen atoms in the POM framework (1.65–2.10), indicating that

these oxygen atoms are monoprotinated to form Co–OH–W fragments. The data of X-ray, elemental, and TG analyses show that the formula of Co2 is TBA₆[Co₂(γ -H₃SiW₁₀O₃₆)₂]·3H₂O. The formation of Co2 from Co-SiW10 can be expressed by eq 2.



Compound Co2 was a γ -Keggin silicotungstate dimer pillared by two cobalt cations. The Co1...Co1* distance was 5.14 Å. Each cobalt cation in Co2 was located “in-pocket” of the vacant site and hexacoordinated by four terminal oxygen atoms (O1, O2, O3*, and O4*), one oxygen atom of the central {SiO₄} tetrahedron (O5), and one edge-sharing oxygen atom (O11). As shown in Figure 5, one of the two vacant sites of each [γ -H₃SiW₁₀O₃₆]⁵⁻ subunit was occupied by a cobalt cation. Up to the present, several γ -Keggin silicotungstate dimers pillared by two metal cations have been reported; for example, [M₂(μ -OH)₂(γ -SiW₁₀O₃₆)₂]ⁿ⁻ (M = Zr⁴⁺, Hf⁴⁺, Dy³⁺, or Gd³⁺),^{3a,17d} [Cu₂(μ -H₂O)(γ -SiW₁₀O₃₆)₂]¹²⁻,^{17c} [RE(acetone)(H₂O)₂]₂(γ -H₂SiW₁₀O₃₆)₂]⁶⁻ (RE = Y³⁺, Nd³⁺, Eu³⁺, Gd³⁺, Tb³⁺, or Dy³⁺),^{17e} and [{PhSn(H₂O)}₂(γ -SiW₁₀O₃₆)₂]¹⁰⁻.^{3b} In the case of POM dimers with bridging hydroxo or aqua ligands between two metal cations, i.e., [M₂(μ -OH)₂(γ -SiW₁₀O₃₆)₂]ⁿ⁻ and [Cu₂(μ -H₂O)(γ -SiW₁₀O₃₆)₂]¹²⁻, the vacant sites of γ -Keggin POM frameworks squarely faced each other.^{3a,17c,d} In contrast, the dimer configurations are slightly slipped without bridging ligands between two metal cations, i.e., [{RE(acetone)(H₂O)}₂]₂(γ -H₂SiW₁₀O₃₆)₂]⁶⁻ and [{PhSn(H₂O)}₂]₂(γ -SiW₁₀O₃₆)₂]¹⁰⁻.^{3b,17e} In the case of Co2, no internal ligands existed between two cobalt cations, and a hydrogen-bonding interaction between O3 and O4* was observed (O3...O4* distance = 2.63 Å),³⁰ probably resulting in the formation of the significantly slipped configuration of Co2 in comparison with the above-mentioned previously reported POM dimers.

The reaction of Co2 with 2 equiv of Co(NO₃)₂ and HNO₃ with respect to Co2 in a mixed solvent of DMF and acetone (1:1, v/v) gave pink precipitates (93% yield based on Co2). The IR and diffuse-reflectance UV/vis spectra of the precipitates were identical with those of Co-SiW10 obtained by the reaction in eq 1 (Figure S4 in the SI), showing that Co2 can reversibly be transformed into the starting Co-SiW10. The transformation can be expressed by eq 3. Thus, Co-SiW10 and Co2 were reversibly transformed by the addition and/or subtraction of required components to Co-SiW10 or Co2, the addition of TBA cations and [γ -SiW₁₀O₃₆]⁸⁻ for Co-SiW10 → Co2, and the addition of cobalt cations and subtraction of TBA cations for Co2 → Co-SiW10 (eqs 2 and 3).



Synthesis and Structure Characterization of Co4 and Reversible Transformation between Co-SiW10 and Co4.

The reaction of Co-SiW10 with 3 equiv of TBAOH with respect to Co-SiW10 in acetone yielded Co4 as purple precipitates (87% yield based on Co-SiW10). By X-ray crystallographic analysis, the molecular structure of Co4

could successfully be determined. The molecular structure of the anion part of **Co4** is represented in Figure 6 (Figure S5 in the SI for ORTEP and Table S3 in the SI for the crystallographic data). The selected bond lengths and angles are summarized in Tables 3 and S4 in the SI.

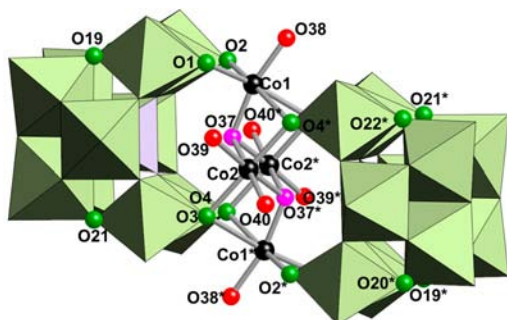


Figure 6. Polyhedral and ball-and-stick representation of the anion part of **Co4** (see Figure S4 in the SI for ORTEP). The $\{WO_6\}$ and $\{SiO_4\}$ units are shown as green octahedra and gray tetrahedra, respectively. Black, red, green, and pink spheres indicate cobalt cations, oxygen atoms of aqua ligands, oxygen atoms of the $\{WO_6\}$ units, and monoprotonated oxygen atoms, respectively. Four protons are possibly disordered on oxygen atoms O19–O22 and O19*–O22*.

Six TBA cations per one **Co4** anion could crystallographically be assigned in accordance with the results of elemental analysis. The BVS values of cobalt (1.85 and 2.07), tungsten (5.99–6.34), and silicon (3.98) atoms in **Co4** indicate that the

respective valences are 2+, 6+, and 4+. The BVS value of O37 was 1.24, showing that O37 is a μ_3 -OH ligand bridging three cobalt cations (Co1, Co2, and Co2*). The oxygen atoms O38, O39, and O40 were aqua ligands (BVS values: 0.38–0.50). Taking the numbers of TBA cations and $[\gamma-SiW_{10}O_{36}]^{8-}$ subunits and the valence of the tetracobalt–oxygen core ($[\{Co(H_2O)\}_2(\mu_3-OH)_2\{Co(H_2O)_2\}_2]^{6+}$) into account, four protons exist per one **Co4** molecule. The BVS values of O19–O22 were in the range of 1.43–1.50 and relatively lower than those of the other oxygen atoms in the POM framework (1.63–2.11). In the reported multimetal-containing γ -Keggin POMs, oxygen atoms of these positions (O19–O22) are protonated to form W–OH–W species.^{17b,f-i} Similarly, in the case of **Co4**, four protons would be disordered on these eight oxygen atoms (O19–O22 and O19*–O22*). The data of X-ray, elemental, and TG analyses show that the formula of **Co4** is $TBA_6[\{Co(H_2O)\}_2(\mu_3-OH)_2\{Co(H_2O)_2\}_2(\gamma-H_2SiW_{10}O_{36})_2] \cdot 5H_2O$. The formation of **Co4** from **Co-SiW10** can be expressed by eq 4. For this transformation, TBAOH was an indispensable component and incorporated into **Co-SiW10**, i.e., TBA cations as countercations and OH^- as coordinating ligands (μ_3 -OH or aqua ligands), resulting in the formation of **Co4**.

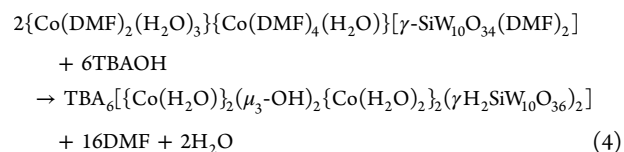
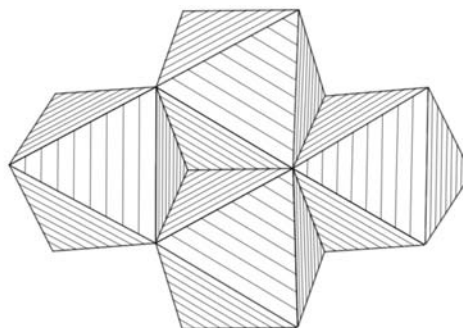
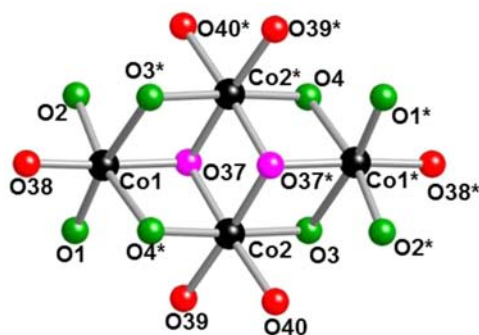


Table 3. Selected Bond Lengths (Å) for Tetracobalt Cores of **Co4** and Reported Compounds (Comparison)^a



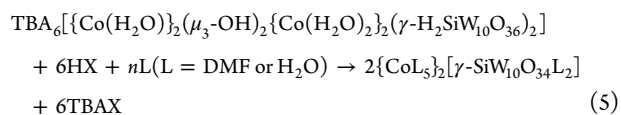
	Co4	$[Co_4(H_2O)(XM_9O_{34})_2]^{n-}$						
		1	X = P; M = W	X = Si; M = W	X = Ge; M = W	X = As; M = W	X = V; M = W	X = Ge; M = Mo
Co1...Co2	3.2085	3.196	3.178	3.183	3.163	3.222	3.232	3.135
Co2...Co2	3.111	3.134	3.305	3.300	3.197	3.384	3.369	3.164
Co1–O37	1.955	2.072	2.17	2.156	2.104	2.145	2.166	2.083
Co1–O1	2.134	2.039	1.99	2.042	2.115	2.054	2.078	2.077
Co1–O2	2.097	2.103	2.10	2.059	2.058	2.073	2.068	2.053
Co1–O3*	2.561	2.110	2.11	2.073	2.108	2.119	2.121	2.107
Co1–O4*	2.448	2.134	2.04	2.114	2.121	2.14	2.109	2.103
Co1–O38	1.950	2.117	2.15	2.063	2.095	2.045	2.121	2.077
Co2–O37	2.064	2.065	2.24	2.235	2.105	2.186	2.198	2.133
Co2–O37*	2.045	2.066	2.17	2.227	2.103	2.197	2.153	2.109
Co2–O3	2.154	2.165	2.01	2.111	2.156	2.109	2.107	2.129
Co2–O4*	2.172	2.167	2.04	2.079	2.160	2.126	2.124	2.133
Co2–O39	2.050	2.053	1.98	1.990	2.024	2.016	2.009	2.036
Co2–O40	2.047	2.092	2.04	1.988	2.022	2.010	1.974	2.023

^a1 = $[Co_4(\mu_3-OH)_2(H_2O)_6(ntp)_2]$ ($H_3ntp = N(CH_2CH_2COOH)_3$). The data of 1 and $[Co(H_2O)(XM_9O_{34})_2]^{n-}$ are taken from refs 35 and 7, respectively.

Compound **Co4** possessed the tetracobalt–oxygen core, $[\{\text{Co}(\text{H}_2\text{O})\}_2(\mu_3\text{-OH})_2\{\text{Co}(\text{H}_2\text{O})\}_2]^{6+}$, sandwiched by two $[\gamma\text{-H}_2\text{SiW}_{10}\text{O}_{36}]^{6-}$ subunits. In the half-unit of $\{\gamma\text{-SiW}_{10}\text{O}_{36}\text{Co}_2(\text{OH})(\text{H}_2\text{O})_3\}$, two cobalt cations (Co1 and Co2) were located “out-of-pocket” of the vacant site in γ -Keggin subunits and corner-shared. Thus, cobalt cations were coordinated to terminal oxygen atoms of γ -Keggin subunits without direct interaction with the internal $\{\text{SiO}_4\}$ tetrahedra. In contrast, cobalt cations in **Co2** were located “in-pocket” of the vacant site, as mentioned in the former section. The anion structure of **Co4** somewhat resembles our previously reported $\text{TBA}_8[\{\text{Zn}(\text{H}_2\text{O})\}_2(\mu_3\text{-OH})_2\{\text{M}(\text{H}_2\text{O})\}_2(\gamma\text{-HSiW}_{10}\text{O}_{36})_2][\text{M}2\text{Zn}2; \text{M} = \text{Co}^{2+} (\text{Co}2\text{Zn}2)^{17a}$ or $\text{Zn}^{2+} (\text{Zn}4);^{17b}$ Table S4 in the SI]. The inner metal cations sandwiched by the lacunary POM subunits in both **Co4** and **M2Zn2** were octahedrally coordinated by two μ_3 -OH ligands (O37 and O37*), two aqua ligands (O39 and O40), and two terminal oxygen atoms of $[\gamma\text{-H}_2\text{SiW}_{10}\text{O}_{36}]^{6-}$ subunits (O3 and O4*). The crucial difference between **Co4** and **M2Zn2** was the coordination of terminal metal cations. The terminal Co1 cation in **Co4** possessed the distorted octahedral geometry with one μ_3 -OH ligand (O37), one aqua ligand (O38), and four terminal oxygen atoms of $[\gamma\text{-H}_2\text{SiW}_{10}\text{O}_{36}]^{6-}$ subunits (O1, O2, O3*, and O4*), while the terminal zinc cations in **M2Zn2** possessed tetrahedral geometry.^{17a,b} The central Co2...Co2* and central-to-terminal Co1...Co2 distances in **Co4** were 3.11 and 3.21 Å, respectively. The bond lengths and angles in the tetracobalt–oxygen core, $[\{\text{Co}(\text{H}_2\text{O})\}_2(\mu_3\text{-OH})_2\{\text{Co}(\text{H}_2\text{O})\}_2]^{6+}$, were similar to those in the previously reported organocobalt complex, $[\text{Co}_4(\mu_3\text{-OH})_2(\text{H}_2\text{O})_6(\text{ntp})_2]$ (**1**; $\text{H}_3\text{ntp} = \text{N}(\text{CH}_2\text{CH}_2\text{COOH})_3$),³⁵ and tetracobalt-containing Weakley-type sandwich POMs, $[\text{Co}_4(\text{H}_2\text{O})_2(\text{XM}_9\text{O}_{34})_2]^{n-}$ ($\text{X} = \text{P}^{5+}, \text{Si}^{4+}, \text{Ge}^{4+}, \text{As}^{5+}$ or V^{5+} ; $\text{M} = \text{Mo}^{6+}$ or W^{6+} ; Table S4 in the SI).⁷

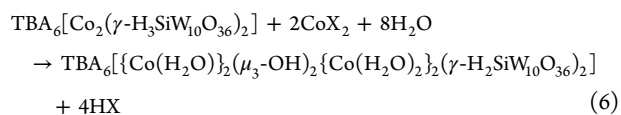
The χT value of **Co4** at 300 K ($12.46 \text{ cm}^3 \text{ K mol}^{-1}$, $\mu_{\text{eff}} = 9.98 \mu_{\text{B}}$; Figure S4b in the SI) was close to that calculated with four Co^{2+} cations upon the independent existence of the spin and orbital momentums ($10.4 \mu_{\text{B}}$), indicating the contribution of the orbital momentum typical for a $^4\text{T}_{1g}$ ground state.^{31,32} The diffuse-reflectance UV/vis spectrum of **Co4** showed three broad bands at 534, 572, and 674 nm (Figure 2d). The bands at 534 and 572 nm are probably due to the central dicobalt–oxygen core, $[\text{Co}_2(\mu\text{-OH})_2]^{2+}$, because similar bands were observed for our previously reported **Co2Zn2** with the same dicobalt–oxygen core (Table S4 in the SI).^{17a,36} The band at 674 nm is probably due to the terminal cobalt cations in the more distorted octahedral environment.

In the former section, the reversible transformation between **Co-SiW10** and **Co2** was demonstrated. Here, the reversible transformation between **Co-SiW10** and **Co4** was investigated. As mentioned above, the addition of TBA cations and OH^- into a solution of **Co-SiW10** gave **Co4** (eq 4). Therefore, we expected that the transformation of **Co4** into **Co-SiW10** is possible by the addition of acids (HX). We attempted to transform **Co4** into **Co-SiW10** in the presence of various kinds of acids. Relatively strong acids such as HNO_3 and HCl promoted transformation; for example, the reaction of **Co4** with 6 equiv of HNO_3 with respect to **Co4** in a mixed solvent of DMF and acetone (1:1, v/v) afforded **Co-SiW10** (91% yield based on **Co4**; Figure S6 in the SI; eq 5). Therefore, the reversible transformation between **Co-SiW10** and **Co4** could be realized (eqs 4 and 5).



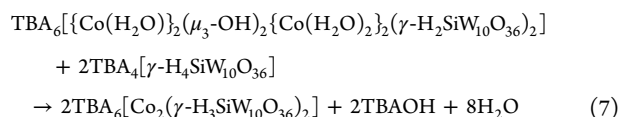
Reversible Transformation between **Co2** and **Co4**.

Finally, the reversible transformation between **Co2** and **Co4** was investigated. Both **Co2** and **Co4** possessed dimeric structures encapsulating cobalt cations (Figures 5 and 6) and six TBA cations, as mentioned in the former sections. We expected that **Co4** can be synthesized by the insertion of additional two cobalt cations into **Co2**. We attempted to transform **Co-SiW10** into **Co4** in the presence of various kinds of sources, and $\text{Co}(\text{acac})_2$ or $\text{Co}(\text{OAc})_2$ ($\text{OAc} = \text{acetate}$) efficiently promoted the transformation in the presence of DMF and water to afford **Co4** [85% yield for $\text{Co}(\text{acac})_2$, 38% yield for $\text{Co}(\text{OAc})_2$ based on **Co2**; Figure S7 in the SI; eq 6]. In contrast, **Co-SiW10** was preferably formed when using $\text{Co}(\text{NO}_3)_2$ or CoCl_2 , which is likely due to promotion of the reaction in eq 3 by the relatively strong acids produced (e.g., HNO_3 and HCl ; eq 6).



Notably, different metals could be introduced into **Co2** according to eq 6. For example, when the reaction of **Co2** with $\text{Zn}(\text{acac})_2$ was carried out, a sandwich-type silicotungstate dimer, $\text{TBA}_8[\{\text{Zn}(\text{H}_2\text{O})\}_2(\mu_3\text{-OH})_2\{\text{Co}(\text{H}_2\text{O})\}_2(\gamma\text{-HSiW}_{10}\text{O}_{36})_2]$ (**Co2Zn2**),¹⁰ could be obtained (78% yield based on **Co2**). X-ray analysis of **Co2Zn2** showed that the cobalt and zinc cations are selectively located at the central and terminal positions, respectively, with their preferable geometries (octahedral for cobalt and tetrahedral for zinc; Figure S8 in the SI).

In addition, **Co4** could successfully be transformed into **Co2** by the addition of required amounts of the γ -Keggin subunits. When the reaction of **Co4** with 2 equiv of $\text{TBA}_4[\gamma\text{-H}_4\text{SiW}_{10}\text{O}_{36}]$ with respect to **Co4** was carried out in the presence of *p*-toluenesulfonic acid (TsOH , 2 equiv), the reaction efficiently proceeded to give **Co2** (74% yield; Figure S9 in the SI). The reaction possibly proceeds according to eq 7, and the role of TsOH is likely to neutralize OH^- formed by the reaction.



CONCLUSIONS

In this work, we have successfully synthesized a novel cobalt salt of a dilacunary γ -Keggin silicotungstate **Co-SiW10** by the reaction of $\text{TBA}_4[\gamma\text{-H}_4\text{SiW}_{10}\text{O}_{36}]$ with 2 equiv of $\text{Co}(\text{NO}_3)_2$ in a mixed solvent of DMF and acetone. Compound **Co-SiW10** could be utilized as a precursor for novel di- and tetracobalt-containing silicotungstate dimers **Co2** and **Co4**. The reversible transformation between these three compounds took place simply by the addition and/or subtraction of required components in appropriate solvents (eqs 2–7; figure in the Abstract).

■ ASSOCIATED CONTENT

■ Supporting Information

Crystallographic data (CIF files) for **Co-SiW10**, **Co2**, and **Co4**, Figures S1–S12, Tables S1–S4, and additional references. This material is available free of charge via the Internet at <http://pubs.acs.org>.

■ AUTHOR INFORMATION

Corresponding Author

*E-mail: tmizuno@mail.ecc.u-tokyo.ac.jp. Tel: +81-3-5841-7272. Fax: +81-3-5841-7220.

Notes

The authors declare no competing financial interest.

■ ACKNOWLEDGMENTS

This work was supported in part by the Japan Society for the Promotion of Science (JSPS) and a Grant-in-Aid for Scientific Research from the Ministry of Education, Culture, Science, Sports, and Technology of Japan (MEXT).

■ REFERENCES

- (1) (a) Sadakane, M.; Steckhan, E. *Chem. Rev.* **1998**, *98*, 219. (b) Zheng, S.-T.; Yang, G.-Y. *Chem. Soc. Rev.* **2012**, *41*, 7623. (c) Mialane, P.; Dolbecq, A.; Sécheresse, F. *Chem. Commun.* **2006**, *33*, 3477. (d) Oms, O.; Dolbecq, A.; Mialane, P. *Chem. Soc. Rev.* **2012**, *41*, 7497. (e) Guo, Y.; Hu, C. *J. Mol. Catal. A: Chem.* **2007**, *262*, 136. (f) Hill, C. L.; Prosser-McCartha, C. M. *Coord. Chem. Rev.* **1995**, *143*, 407. (g) Okuhara, T.; Mizuno, N.; Misono, M. *Adv. Catal.* **1996**, *41*, 113. (h) Neumann, R. *Prog. Inorg. Chem.* **1998**, *47*, 317. (i) Thematic issue on polyoxometalates: Hill, C. L. *Chem. Rev.* **1998**, *98*, 1. (j) Kozhevnikov, I. V. *Catalysis by Polyoxometalates*; John Wiley & Sons, Ltd.: Chichester, U.K., 2002. (k) Mizuno, N.; Yamaguchi, K.; Kamata, K. *Coord. Chem. Rev.* **2005**, *249*, 1944.
- (2) (a) Biboum, R. N.; Njiki, C. P. N.; Zhang, G.; Kortz, U.; Mialane, P.; Dolbecq, A.; Mbomekalle, I. M.; Nadjo, L.; Keita, B. *J. Mater. Chem.* **2011**, *21*, 645. (b) Yin, Q.; Tan, J. M.; Besson, C.; Geletii, Y. V.; Musaev, D. G.; Kuznetsov, A. E.; Luo, Z.; Hardcastle, K. I.; Hill, C. L. *Science* **2010**, *328*, 342.
- (3) (a) Yamaguchi, S.; Kikukawa, Y.; Tsuchida, K.; Nakagawa, Y.; Uehara, K.; Yamaguchi, K.; Mizuno, N. *Inorg. Chem.* **2007**, *46*, 8502. (b) Xin, F.; Pope, M. T. *Inorg. Chem.* **1996**, *35*, 5693. (c) Geletii, Y. V.; Botar, B.; Kögerler, P.; Hillesheim, D. A.; Musaev, D. G.; Hill, C. L. *Angew. Chem., Int. Ed.* **2008**, *47*, 3896. (d) Kamata, K.; Yamaguchi, S.; Kotani, M.; Yamaguchi, K.; Mizuno, N. *Angew. Chem., Int. Ed.* **2008**, *47*, 2407. (e) Kikukawa, Y.; Yamaguchi, S.; Nakagawa, Y.; Uehara, K.; Uchida, S.; Yamaguchi, K.; Mizuno, N. *J. Am. Chem. Soc.* **2008**, *130*, 15872. (f) Nakagawa, Y.; Kamata, K.; Kotani, M.; Yamaguchi, K.; Mizuno, N. *Angew. Chem., Int. Ed.* **2005**, *44*, 5136.
- (4) (a) El Moll, H.; Dolbecq, A.; Marrot, J.; Rousseau, G.; Haouas, M.; Taulelle, F.; Rogez, G.; Wernsdorfer, W.; Keita, B.; Mialane, P. *Chem.—Eur. J.* **2012**, *18*, 3845. (b) Lydon, C.; Sabi, M. M.; Symes, M. D.; Long, D.-L.; Murrie, M.; Yoshii, S.; Nojiri, H.; Cronin, L. *Chem. Commun.* **2012**, *48*, 9819. (c) Ibrahim, M.; Lan, Y.; Bassil, B. S.; Xiang, Y.; Suchopar, A.; Powell, A. K.; Kortz, U. *Angew. Chem., Int. Ed.* **2011**, *50*, 4708.
- (5) (a) Clemente-Juan, J. M.; Coronado, E.; Galán-Mascarós, J. R.; Gómez-García, C. J. *Inorg. Chem.* **1999**, *38*, 55. (b) Botar, B.; Kögerler, P.; Hill, C. L. *Inorg. Chem.* **2007**, *46*, 5398. (c) Wu, Q.; Li, Y.-G.; Wang, Y.-H.; Wang, E.-B.; Zhang, Z.-M.; Clérac, R. *Inorg. Chem.* **2009**, *48*, 1606.
- (6) (a) El Weakley, T. J. R.; Malik, S. A. *J. Inorg. Nucl. Chem.* **1967**, *29*, 2935. (b) Liu, J.; Ortéga, F.; Sthuraman, P.; Katsoulis, D. E.; Costello, C. E.; Pope, M. T. *J. Chem. Soc., Dalton Trans.* **1992**, 1901. (c) Weakley, T. J. R. *Polyhedron* **1987**, *6*, 931.
- (7) (a) Evans, H. T.; Tourné, C. M.; Tourné, G. F.; Weakley, T. J. R. *J. Chem. Soc., Dalton Trans.* **1986**, 2699. (b) Zhang, L.-Z.; Gu, W.; Liu, X.; Dong, Z.; Yang, Y.-S.; Li, B.; Liao, D.-Z. *Inorg. Chem. Commun.* **2007**, *10*, 1378. (c) Wang, J.; Ma, P.; Shen, Y.; Niu, J. *Cryst. Growth Des.* **2008**, *8*, 3130. (d) Weakley, T. J. R. *Acta Crystallogr., Sect. C* **1997**, *53*, IUC9700025. (e) Li, B.; Yan, Y.; Li, F.; Xu, L.; Bi, L.; Wu, L. *Inorg. Chim. Acta* **2009**, *362*, 2796. (f) Li, S.; Zhao, J.; Ma, P.; Du, J.; Niu, J.; Wang, J. *Inorg. Chem.* **2009**, *48*, 9819.
- (8) (a) Ruhlmann, L.; Canny, J.; Vaissermann, J.; Thouvenot, R. *Dalton Trans.* **2004**, 794. (b) Finke, R. G.; Droegge, M. W. *Inorg. Chem.* **1983**, *22*, 1006.
- (9) Zhu, G.; Geletii, Y. V.; Song, J.; Zhao, C.; Glass, E. N.; Bacsá, J.; Hill, C. L. *Inorg. Chem.* **2013**, *52*, 1018.
- (10) Lv, H.; Song, J.; Gelletii, Y. V.; Guo, W.; Bacsá, J.; Hill, C. L. *Eur. J. Inorg. Chem.* **2013**, 1720.
- (11) Bassil, B. S.; Ibrahim, M.; Mal, S. S.; Suchopar, A.; Biboum, R. N.; Keita, B.; Nadjo, L.; Nellutla, S.; van Tol, J.; Dalal, N. S.; Kortz, U. *Inorg. Chem.* **2009**, *49*, 4949.
- (12) (a) Chen, L.; Shi, D.; Zhao, J.; Wang, Y.; Ma, P.; Niu, J. *Inorg. Chem. Commun.* **2011**, *14*, 1052. (b) Peng, J.; Ma, H.-Y.; Han, Z.-G.; Dong, B.-X.; Li, W.-Z.; Lu, J.; Wang, E.-B. *Dalton Trans.* **2003**, 3850.
- (13) (a) Liu, X.; Gao, G.; Xu, L.; Li, F.; Liu, L.; Jiang, N.; Yang, Y. *Solid State Sci.* **2009**, *11*, 1433. (b) Fukaya, K.; Yamase, T. *Bull. Chem. Soc. Jpn.* **2007**, *80*, 178. (c) Galán-Mascarós, J. R.; Gómez-García, C. J.; Borrás-Almenar, J. J.; Coronado, E. *Adv. Mater.* **1994**, *6*, 221. (d) Gao, J.; Yan, J.; Beeg, S.; Long, D.-L.; Cronin, L. *J. Am. Chem. Soc.* **2013**, *1135*, 1796.
- (14) (a) Gabb, D.; Pradeep, C. P.; Miras, H. N.; Mitchell, S. G.; Long, D.-L.; Cronin, L. *Dalton Trans.* **2012**, *41*, 10000. (b) Ruhlmann, L.; Canny, J.; Contant, R.; Thouvenot, R. *Inorg. Chem.* **2002**, *41*, 3811. (c) Yao, S.; Zhang, Z.; Li, Y.; Wang, E. *Dalton Trans.* **2010**, 39, 3884.
- (15) (a) Nsouli, N. H.; Ismail, A. H.; Helgadottir, I. S.; Dickman, M. H.; Clemente-Juan, J. M.; Kortz, U. *Inorg. Chem.* **2009**, *48*, 5884. (b) Mitchell, S. G.; Ritchie, C.; Long, D.-L.; Cronin, L. *Dalton Trans.* **2008**, 1415. (c) Lisnard, L.; Mialane, P.; Dolbecq, A.; Marrot, J.; Clemente-Juan, J. M.; Coronado, E.; Keita, B.; de Oliveira, P.; Nadjo, L.; Sécheresse, F. *Chem.—Eur. J.* **2007**, *13*, 3525. (d) Bassil, B. S.; Nellutla, S.; Kortz, U.; Stow, A. C.; van Tol, J.; Dalal, N. S.; Keita, B.; Nadjo, L. *Inorg. Chem.* **2005**, *44*, 2659. (e) Bassil, B. S.; Kortz, U.; Tigan, A. S.; Clemente-Juan, J. M.; Keita, B.; de Oliverira, P.; Nadjo, L. *Inorg. Chem.* **2005**, *44*, 9360. (f) Chen, L.; Shi, D.; Zhao, J.; Wang, Y.; Ma, P.; Wang, J.; Niu, J. *Cryst. Growth Des.* **2011**, *11*, 1913. (g) Thiel, J.; Rthie, C.; Miras, H. N.; Streb, C.; Mitchell, S. G.; Boyd, T.; Ochoa, M. N. C.; Rosnes, M. H.; McIver, J.; Long, D.-L.; Cronin, L. *Angew. Chem., Int. Ed.* **2010**, *49*, 6984. (h) Tan, R.; Pang, X.; Wang, H.; Cui, S.; Jiang, Y.; Wang, C.; Wang, X.; Song, W. *Inorg. Chem. Commun.* **2012**, *25*, 70. (i) Rousseau, G.; Oms, O.; Dolbecq, A.; Marrot, J.; Mialane, P. *Inorg. Chem.* **2011**, *50*, 7376. (j) Zhao, X.; Li, Y.-G.; Wang, Y.-H.; Wang, E.-B. *Transition Met. Chem.* **2008**, *33*, 323. (k) Zhang, Z.; Wang, E.; Li, Y.; An, H.; Qi, Y.; Xu, L. *J. Mol. Struct.* **2008**, *872*, 176. (l) Zhang, Z.; Qi, Y.; Wang, E.; Li, Y.; Tan, H. *Inorg. Chim. Acta* **2008**, *361*, 1797.
- (16) (a) Bassil, B. S.; Dickman, M. H.; Reicke, M.; Kortz, U.; Keita, B.; Nadjo, L. *Dalton Trans.* **2006**, 4253. (b) Liu, H.; Peng, J.; Su, Z.; Chen, Y.; Dong, B.; Tian, A.; Han, Z.; Wang, E. *Eur. J. Inorg. Chem.* **2006**, 4827.
- (17) (a) Suzuki, K.; Kikukawa, Y.; Uchida, S.; Tokoro, H.; Imoto, K.; Ohkoshi, S.; Mizuno, N. *Angew. Chem., Int. Ed.* **2012**, *51*, 1597. (b) Kikukawa, Y.; Yamaguchi, K.; Mizuno, N. *Angew. Chem., Int. Ed.* **2010**, *49*, 6096. (c) Suzuki, K.; Shinoue, M.; Mizuno, N. *Inorg. Chem.* **2012**, *51*, 11574. (d) Suzuki, K.; Sato, R.; Mizuno, N. *Chem. Sci.* **2013**, *4*, 596. (e) Suzuki, K.; Sugawa, M.; Kikukawa, Y.; Kamata, K.; Yamaguchi, K.; Mizuno, N. *Inorg. Chem.* **2012**, *51*, 6953. (f) Kikukawa, Y.; Kuroda, Y.; Suzuki, K.; Hibino, M.; Yamaguchi, K.; Mizuno, N. *Chem. Commun.* **2013**, 49, 376. (g) Hirano, T.; Uehara, K.; Kamata, K.; Mizuno, N. *J. Am. Chem. Soc.* **2012**, *134*, 6425. (h) Kikukawa, Y.; Suzuki, K.; Sugawa, M.; Hirano, T.; Kamata, K.; Yamaguchi, K.; Mizuno, N. *Angew. Chem., Int. Ed.* **2012**, *51*, 3686. (i) Kikukawa, Y.; Kuroda, Y.; Yamaguchi, K.; Mizuno, N. *Angew. Chem., Int. Ed.* **2012**, *51*, 2434.

(18) Cyclic voltammograms for **Co-SiW10**, **Co2**, and **Co4** are shown in Figures S10 and S11 in the SI.

(19) (a) Kamata, K.; Yonehara, K.; Sumida, Y.; Yamaguchi, K.; Hikichi, S.; Mizuno, N. *Science* **2003**, *300*, 964. (b) Sugahara, K.; Kuzuya, S.; Hirano, T.; Kamata, K.; Mizuno, N. *Inorg. Chem.* **2012**, *51*, 7932.

(20) (a) *CrystalClear*, version 1.3.6; Rigaku and Rigaku/MS: The Woodlands, TX. (b) Pflugrath, J. W. *Acta Crystallogr.* **1999**, *D55*, 1718.

(21) Otwinowski, Z.; Minor, W. Processing of X-ray Diffraction Data Collected in Oscillation Mode. In *Methods in Enzymology*; Carter, C. W., Jr., Sweet, R. M., Eds.; Macromolecular Crystallography, Part A; Academic Press: New York, 1997; Vol. 276, pp 307–326.

(22) *CrystalStructure*, version 3.8; Rigaku and Rigaku/MS: The Woodlands, TX.

(23) Farrugia, L. J. *J. Appl. Crystallogr.* **1999**, *32*, 837.

(24) Sheldrick, G. M. *SHELX97, Programs for Crystal Structure Analysis*, release 97-2; University of Göttingen: Göttingen, Germany, 1997.

(25) (a) Chen, H.; Ding, Y.; Xu, X.; Wang, E.; Chen, W.; Chang, S.; Wang, X. *J. Coord. Chem.* **2009**, *62*, 347. (b) Niu, J.-Y.; Guo, D.-J.; Wang, J.-P.; Zhao, J.-W. *Cryst. Growth Des.* **2004**, *4*, 241. (c) Zhao, J. W.; Zhang, X. F.; Ma, P. T.; Feng, Y. Q.; Wang, J. P.; Niu, J. Y. *Russ. J. Coord. Chem.* **2009**, *35*, 891. (d) Wang, J.; Li, J.; Niu, J. *Sci. China B* **2006**, *49*, 437. (e) Niu, J.; Zhao, J.; Wang, J.; Ma, P. *J. Mol. Struct.* **2004**, *699*, 85. (f) Wang, J.; Wu, Q.; Niu, J. *Sci. China B* **2002**, *45*, 647. (g) Wang, J.; Zhao, J.; Niu, J.; Guo, D.; Dang, D. *Sci. China B* **2003**, *46*, 583. (h) Wang, J.; Duan, X.; Niu, J. *J. Mol. Struct.* **2004**, *693*, 187. (i) Zhao, W.-F.; Zou, C.; Shi, L.-X.; Yu, J.-C.; Qian, G.-D.; Wu, C.-D. *Dalton Trans.* **2012**, *41*, 10091. (j) Wang, J.-P.; Zhao, J.-W.; Duan, X.-Y.; Niu, J.-Y. *Cryst. Growth Des.* **2006**, *6*, 507. (k) Wang, J.; Li, J.; Niu, J. *J. Coord. Chem.* **2005**, *58*, 1639. (l) Wang, Y.; Xu, L.; Jiang, N.; Zhao, L.; Li, F.; Liu, X. *CrystEngComm* **2011**, *13*, 410.

(26) Lever, A. B. P. *Inorganic Electronic Spectroscopy*, 2nd ed.; Elsevier: Amsterdam, The Netherlands, 1984.

(27) Brown, I. D.; Altermatt, D. *Acta Crystallogr.* **1985**, *B41*, 244.

(28) The γ -Keggin $[\gamma\text{-XW}_{10}\text{O}_{36}]^{n-}$ frameworks essentially possess C_{2v} symmetry.^{3,17} When four axial oxygen atoms at the vacant site are not equivalent, distortion of the frameworks takes place, resulting in decreasing symmetry.^{19a}

(29) (a) Canny, J.; Tézé, A.; Thouvenot, R.; Hervé, G. *Inorg. Chem.* **1986**, *25*, 2114. (b) Hartl, H.; Hubert, V. *Acta Crystallogr.* **1996**, *C52*, 757.

(30) Pimentel, G. C.; McClellan, A. L. *The Hydrogen Bond*; W. H. Freeman and Company: San Francisco, 1960.

(31) The XRD patterns of polycrystalline samples of **Co2** and **Co4** used for magnetic measurements were in good agreement with the calculated ones using their single crystals. In the case of **Co-SiW10**, the XRD pattern of the polycrystalline sample was mostly consistent with the calculated one using the single-crystal X-ray analysis data (Figure S12 in the SI). Besides the calculated pattern, weak diffraction lines were also observed [ca. 5% estimated by the intensity ratio of the main signals at $2\theta = 5.2^\circ$ for **Co-SiW10** and $2\theta = 5.8^\circ$ for **Co-SiW10-des** (see below)]. In the separate experiments, we confirmed that the new weak diffraction lines were assigned to the compound (**Co-SiW10-des**) obtained by desorption of solvent molecules from **Co-SiW10** and that the molecular structure of **Co-SiW10-des** was the same as that of **Co-SiW10** by IR. In the case of **Co-SiW10-des**, the intramolecular Co...Co distance was 13.9 Å and the shortest intermolecular Co...Co distance was 7.25 Å, also suggesting that the magnetic interaction between cobalt atoms in **Co-SiW10-des** can be neglected.

(32) It was confirmed by XRD analyses that their structures were preserved after the magnetic measurements (Figure S12 in the SI).

(33) The following parameters were obtained for the best fitting (Figure 4a); $g_z = 6.77$, $g_x = 2.74$, $\chi_{\text{TIP}} = 249 \times 10^{-6} \text{ cm}^3 \text{ mol}^{-1}$, and $D = 361.5 \text{ cm}^{-1}$, where g_x and g_z are the anisotropic g factors, χ_{TIP} is temperature-independent paramagnetism, and D is the zero-field splitting. Sakiyama, H. *Inorg. Chim. Acta* **2006**, *359*, 2097.

(34) The weak antiferromagnetic interaction between two Co^{2+} cations in **Co2** was observed, and the following parameters were

obtained for the best fitting (Figure 4b): $J = -0.13 \text{ cm}^{-1}$, $g_z = 2.19$, $g_x = 4.94$, $\chi_{\text{TIP}} = 148 \times 10^{-6} \text{ cm}^3 \text{ mol}^{-1}$, and $D = 102.8 \text{ cm}^{-1}$, where J is the exchange interaction parameter between Co^{2+} cations.

(35) King, P.; Clérac, R.; Wernsdorfer, W.; Anson, C. E.; Powell, A. K. *Dalton Trans.* **2004**, 2670.

(36) The bands at 534 and 572 nm were red-shifted by ca. 50 nm from those of **Co2Zn2**.^{17a}